Sensitivity analysis for the design and operation of a non-contacting mechanical face seal

J Dayan, M Zou and I Green*
The George W. Woodruff School of Mechanical Engineering, Georgia Institute of Technology, Atlanta, Georgia, USA

Abstract: Detection and diagnosis of failure in non-contacting mechanical face seals may prevent catastrophes in some critical applications. Seal failure due to face contact may occur because of large relative misalignment between the seal rotor and stator faces. The objective of this work is to study the sensitivity of the relative misalignment to changes in the design and operational parameters of a non-contacting flexibly mounted rotor (FMR) mechanical face seal. These sensitivities can be efficiently exploited to prevent possible contact through proper selection of the seal parameters and working point in both the design and the control stages. Among the design parameters, the seal coning angle is by and large independent of other design requirements and should be properly selected to avoid contact. The operational variables greatly influencing the relative misalignment are the clearance, the bearing fluid pressure and the shaft speed. Where active control is considered, the relative misalignment sensitivity to changes in the control parameters should determine the working point. The sensitivity analysis is demonstrated using the data of an existing seal test rig.

Keywords: non-contacting mechanical face seal, sensitivity, parameter analysis, control

NOTATION

$\mathbf{A}$	matrix defined in equation (9)
$\mathbf{C}$	matrix defined in equation (9)
C_o	maintained clearance
D^*	damping coefficient
$\boldsymbol{F}$	set of governing equations [equation (7)]
I^*, I_z^*	rotor transverse and polar moments of inertia
K^*	stiffness coefficient
m^*	rotor mass
P^*	fluid pressure
r^*	radial coordinate
R	dimensionless radial coordinate $= r/r_o$
$\boldsymbol{s}$	sensitivity vector [equation (5)]
$\vec{\boldsymbol{s}}$	non-normalized sensitivity vector (Table 3)
S	seal parameter $= 6\mu\omega(r_o/C_o)^2(1-R_i)^2$
$\mathbf{S}$	elementary sensitivity matrix [equation (6)]
$\boldsymbol{x}$	dimensional input vector [equation (3)]
$\boldsymbol{y}$	dimensionless dependent vector [equation (2)]
β^*	face coning angle
γ^*	misalignment
ΔP_{io}	pressure drop across the liquid film
μ	viscosity
ω	shaft rotating speed

The MS was received on 25 February 1999 and was accepted after revision for publication on 5 July 1999.
**Corresponding author: The GWW School of Mechanical Engineering, Georgia Institute of Technology, Atlanta, GA 30332-0405, USA.*

Subscripts

cr	critical
f	fluid film
i	inner radius
m	mean
o	outer radius
r	rotor
ri	initial rotor misalignment
rI	rotor response to initial misalignment
s	support
33	axial

Superscripts

*	dimensional, non-normalized variable

Definitions

$D_{33} = D_{s33} + D_{f33}$
total axial damping coefficient

$D_{f33} = 4\pi R_m G_o$
film axial damping coefficient

$D_s^* = \frac{1}{2} D_{s33}^* r_s^2$
dimensional support angular damping coefficient

$$E_o = \frac{1 - R_i}{2 + \beta(1 - R_i)}$$
stiffness parameter

$$G_o = \frac{\ln[1 + \beta(1 - R_i)] - [2(1 - R_i)]/[2 + \beta(1 - R_i)]}{\beta^3(1 - R_i)^2}$$
damping parameter

$K = K_s + K_f$
total angular stiffness coefficient

$K_{f33} = 2\pi\Delta P\beta E_o^2/R_m$
film axial stiffness coefficient

$K_{33} = K_{s33} + K_{f33}$
total axial stiffness coefficient

$K_s^* = \frac{1}{2}K_{s33}^* r_s^2$
dimensional support angular stiffness coefficient

$m = m^*\omega^2 C_o/(Sr_o^2)$
dimensionless mass

$\beta = \beta^* r_o/C_o$
dimensionless coning

$\gamma = \gamma^* r_o/C_o$
dimensionless misalignment

Definition of vector y [equation (2)]

$y_1 = D_f = 2\pi R_m^3 G_o$
film angular damping coefficient

$y_2 = D_s = D_s^*\omega C_o/(Sr_o^4)$
support angular damping coefficient

$y_3 = I = I^*\omega^2 C_o/(Sr_o^4)$
transverse moment of inertia

$y_4 = I_z = I_z^*\omega^2 C_o/(Sr_o^4)$
polar moment of inertia

$y_5 = K_f = \pi\Delta P(\beta R_i - 1)E_o^2$
film angular stiffness coefficient

$y_6 = K_s = K_s^* C_o/(Sr_o^4)$
support angular stiffness coefficient

1 INTRODUCTION

A rotating shaft seal is used to separate regions containing two different fluids, as in cooling pumps or compressors of powered vessels. Mechanical face seals are usually composed of two plane face rings, a secondary seal, a compression spring and a drive mechanism (Fig. 1). The two plane face rings are arranged perpendicular to the axis of a rotating shaft to seal the fluid contained in the housing where the shaft penetrates. One ring is attached to the housing and the other is attached to the shaft. In general, one of the two rings is rigidly mounted (mating ring) and the other is flexibly mounted (primary ring), allowing axial and angular freedom of this ring. It is a flexibly mounted rotor (FMR) mechanical face seal when the primary ring is attached to the shaft [**1**] and a flexibly mounted stator (FMS) mechanical face seal when the primary ring is attached to the housing [**2**]. In rotating machinery operating at high speeds and pressures, the seals are made to work in a non-contacting mode for longer life and reliable operation.

The dynamic model of a non-contacting FMR mechanical face seal together with its stability analysis and its steady state response were obtained analytically by Green [**1**, **3**]. He also calculated the rotor behaviour near an equilibrium point in response to small perturbations. A major assumption of the analysis is that there is no contact between the rotor and the stator. However, such face contact may occur during operation owing to large relative misalignment between the seal faces, which operate normally at a small clearance of just a few micrometres [**4**]. Seal face contact, which is not easy to predict, increases the friction and wear of the seal faces. The heat generated by prolonged face contact can cause face deformation and alter the intended seal function. If the contact is left uncontrolled, it may eventually cause seal failure which may be catastrophic in critical applications such as nuclear reactor cooling pumps.

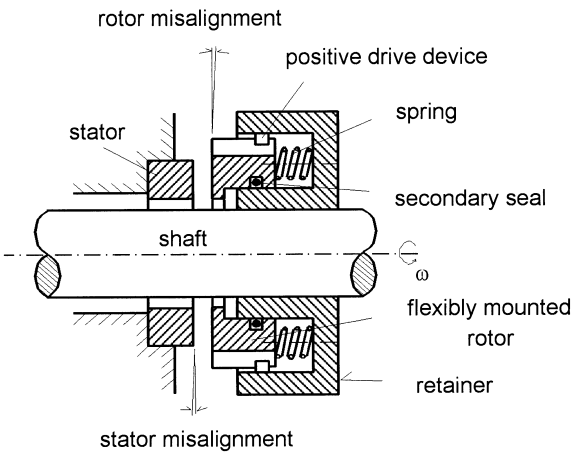

Fig. 1 Scheme of the non-contacting FMR mechanical face seal

It is therefore important to prevent seal face contact, which can be achieved by proper design for most of the common applications, i.e. selecting the parameters of the seal in such a way that it will not be sensitive to changes in the operational variables about its nominal working point. However, in some cases, the working conditions or the applied disturbances may vary substantially, causing large misalignment, beyond what rigid design (no matter how robust) can rectify. In such cases, one or more of the operational variables (clearance, pressure and speed) can be used actively to control the seal behaviour [**5**, **6**].

Three operational variables can be used to control and reduce the misalignment and eliminate the possibility of contact: the clearance between the rotor and the stator faces, the seal differential pressure and the shaft speed. In some applications, one or two of these are fixed, leaving only one controllable variable. Other parameters may help in eliminating a contact, but these have to be accounted for in the original design because they are not subject to variations during operation (geometrical measures, material and structural properties, etc.). In the present paper, the effects of all the design and operational parameters on the seal behaviour are discussed, and the possibility of eliminating undesired contact by reducing the relative misalignment between the faces is considered.

2 PARAMETER ANALYSIS

2.1 Seal axial dynamic model

To perform a sensitivity analysis, the Green [**3**] dynamic mathematical model is adopted. The seal rotor has three degrees of freedom: one axial translation along the shaft axis and two angular rotations about its two inertial axes perpendicular to the shaft axis of rotation (Fig. 1). Theoretically, it was shown that the angular mode is decoupled from the axial mode when motions are limited to small perturbations, and that the equation of motion for the FMR seal can be linearized.

Green [**1**] further pointed out that the stator misalignment, γ_s, and the initial rotor misalignment, γ_{ri}, act as forcing functions to the seal rotor, and he calculated the steady-state solution for the dynamic model in terms of static transmissibility, γ_o/γ_s, and dynamic transmissibility, γ_{rI}/γ_{ri}. The static transmissibility is defined as the ratio between the relative misalignment, γ_o, and the stator misalignment, γ_s. The dynamic transmissibility is defined as the ratio between the relative misalignment, γ_{rI}, and the initial rotor misalignment, γ_{ri}.

Assuming that superposition is valid for small perturbations about the working point (the nominal design point at steady state), the total relative misalignment between the rotor and stator, $\boldsymbol{\gamma}$, is the vector sum of the rotor response to both the stator misalignment and the initial rotor misalignment. The maximum of the total relative misalignment is a cause for concern, and is given by [**1**]

$$\gamma = \gamma_s \sqrt{\frac{K_s^2 + D_s^2}{(K_f + K_s)^2 + (D_s + \frac{1}{2} D_f)^2}} + \gamma_{ri} \sqrt{\frac{K_s^2}{(I_z - I + K_f + K_s)^2 + \left(\frac{1}{2} D_f\right)^2}} \tag{1}$$

In addition to the stator and the initial rotor misalignments, the following parameters also affect the total relative misalignment: the fluid film angular stiffness and damping coefficients (K_f, D_f), the support angular stiffness and damping coefficients (K_s, D_s) and the rotor polar and transverse moments of inertia (I_z and I). These six parameters, defined in the Notation, are considered to be the governing seal properties [**1**, **4**]. In this study they comprise the dependent non-dimensional vector $\boldsymbol{y}$:

$$\boldsymbol{y} = [D_f \quad D_s \quad I \quad I_z \quad K_f \quad K_s] \tag{2}$$

The governing seal properties are functions of the basic physical variables that comprise the vector $\boldsymbol{x}$ of the dimensional input variables:

$$\boldsymbol{x} = [\gamma_{ri}^* \; \gamma_s^* \; \omega \; C_o^* \; \Delta P_{oi}^* \; r_o \; r_i \; \beta^* \; r_s \; \mu \; K_{s33}^* \; D_{s33}^* \; I^* \; I_z^*] \tag{3}$$

The relations between the dependent parameters of vector $\boldsymbol{y}$, the definitions of the various normalized and non-dimensional parameters and the independent parameters of vector $\boldsymbol{x}$ are consistent with Green [**1**] and summarized in the notation. Values and measures of the $\boldsymbol{x}$ vector components used in the numerical example are taken from a seal test rig [**7**, **8**] and are given in Table 1.

Obviously [equation (1)], reducing the stator and initial rotor misalignment will reduce the relative misalignment. Similarly, the qualitative effects of the other parameters can be observed directly from equation (1). The fluid film angular stiffness and damping coefficients strongly affect the total relative misalignment. Increasing these two coefficients will decrease the total relative misalignment. On the other hand, the effect of the rotor polar and transverse moments of inertia is negligible, especially at low shaft speed. The parameters of equation (1), namely the seal properties of vector $\boldsymbol{y}$ [equation (2)], are affected by two kinds of variables:

(a) the seal geometry, e.g. the seal inner and outer diameters and the seal coning angle;
(b) the seal operational variables, such as seal fluid viscosity, fluid pressure, shaft speed and seal clearance.

When the seal is properly designed with a coning angle larger than the critical value, $\beta_{cr} = 1/R_i$ [**3**], the film thickness is minimum at the inside radius of the seal where face contact due to the misalignment might first

Table 1 Values of the input variables for the experimental FMR testing rig

Variable	Value or definition	Units	Description
γ^*_{ri}	0.0015	rad	Rotor initial misalignment
γ^*_s	0.001	rad	Stator misalignment
ω	80–360	rad/s	Shaft speed
C_o	2–10	μm	Design seal clearance
ΔP_{oi}	100–900	kPa	Seal pressure difference
r_o	0.0254	m	Rotor outer radius
r_i	0.0203	m	Rotor inner radius
β^*	0.1–10.0	mrad	Seal coning angle
r_s	0.0206	m	O-ring support radius
μ	0.000894	Pa s	Water viscosity
K^*_s	$5.346 + 146.1\omega^2/(36.36 + \omega^2)$	N m/rad	Support angular stiffness [**8**]
D^*_s	$881.4/(36.6+\omega^2)$	N m s/rad	Support angular damping [**8**]
I^*	0.000375	kg m^2	Rotor transverse moment of inertia
I^*_z	0.000649	kg m^2	Rotor polar moment of inertia

occur. The condition for face contact in terms of the normalized relative misalignment between the seal faces, γ, is [**1**]

$$\gamma = \gamma_{cr} = \frac{1}{R_i} \tag{4}$$

Thus, in order to avoid the possibility of contact between the seal faces, the design and operation should ensure $\gamma < \gamma_{cr}$ at all times.

Studying the effect of the different input variables on the total relative misalignment may suggest a way of selecting the proper design and possible control parameters for a particular application. There are two general cases:

(a) a common case where the seal is operated in a fixed regime of constant speed, constant axial load and minimal disturbances;
(b) a varying operational conditions case, where some of the conditions may change with time (load and speed are the typically varying parameters).

For the first case, where active control is not desired, a proper selection of the design parameters (well within the nominal range satisfying non-contacting requirements) will usually be the ultimate solution. On the other hand, the case of varying conditions may call for a more sophisticated approach. Again, two possible cases may be identified. If axial load and/or speed change within a narrow a priori known range, the proper design approach is to select the parameters in such a way that the nominal working point lies within the safe region and should not be sensitive to changes in the varying parameters. However, if the system may be subject to large changes and possible large disturbances, active control may be needed and the proper design point will be that where it is the most sensitive to changes in the sought control variables.

2.2 Parameter sensitivity study

Since the possibility of getting a contact in the seal is directly proportional to its degree of relative misalignment, the sensitivity of the total relative misalignment, γ, with respect to the input variables affecting this misalignment is sought. The sensitivity vector, $\boldsymbol{s}_{1\times m}$, denotes the sensitivity of γ with respect to each of the m components of the vector of independent input variables, $\boldsymbol{x}$, and is defined as

$$\boldsymbol{s} = \left[\frac{\mathrm{d}\gamma/\gamma}{\mathrm{d}\boldsymbol{x}/\boldsymbol{x}}\right]_{(\boldsymbol{x}^o, \boldsymbol{y}^o)} = \left(\frac{\mathrm{d}\gamma}{\mathrm{d}\boldsymbol{x}} \cdot \frac{\boldsymbol{x}}{\gamma}\right)_{(\boldsymbol{x}^o, \boldsymbol{y}^o)} \tag{5}$$

where $(\boldsymbol{x}^o, \boldsymbol{y}^o)$ are the design values of the independent and the dependent vectors respectively.

Assuming that a continuous solution of the n model equations $\boldsymbol{y} = \boldsymbol{y}(\boldsymbol{x})$ exists, the non-normalized sensitivity is given by

$$\left(\frac{\mathrm{d}\gamma}{\mathrm{d}\boldsymbol{x}}\right)_{1\times m} = \underbrace{\left(\frac{\partial\gamma}{\partial\boldsymbol{x}}\right)_{1\times m}}_{\text{direct effect}} + \underbrace{\left(\frac{\partial\gamma}{\partial\boldsymbol{y}}\right)_{1\times n} \cdot \left(\frac{\partial\boldsymbol{y}}{\partial\boldsymbol{x}}\right)_{n\times m}}_{\text{indirect effect}} \tag{6}$$

where $\boldsymbol{S} = \partial\boldsymbol{y}/\partial\boldsymbol{x}$ is the $n \times m$ matrix of the elementary sensitivity coefficients.

The definitions of the n dependent variables $\boldsymbol{y}$ as the physical governing equations of the system can be written as

$$\boldsymbol{F}(\boldsymbol{x}, \boldsymbol{y}) = \boldsymbol{y} - \boldsymbol{y}(\boldsymbol{x}) = \boldsymbol{0} \tag{7}$$

Matrix **S** can be calculated directly by differentiating the physical governing properties (the definitions of the variables in equation (2)—see the Notation) with respect to $\boldsymbol{x}$:

$$\frac{\partial\boldsymbol{F}}{\partial\boldsymbol{x}} + \frac{\partial\boldsymbol{F}}{\partial\boldsymbol{y}}\frac{\partial\boldsymbol{y}}{\partial\boldsymbol{x}} = 0 \tag{8}$$

Equation (8) is the forward sensitivity equation and this method of obtaining **S** is referred to as the sensitivity direct approach (SDA).

Defining $\mathbf{A} = \partial\boldsymbol{F}/\partial\boldsymbol{y}$ and $\mathbf{C} = -\partial\boldsymbol{F}/\partial\boldsymbol{x}$, equation (8) can be written as

$$\mathbf{AS} = \mathbf{C} \tag{9}$$

The differentiation of $\partial \boldsymbol{F}/\partial \boldsymbol{x}$ and $\partial \boldsymbol{F}/\partial \boldsymbol{y}$ is carried out, $\mathbf{A}$ and $\mathbf{C}$ are evaluated and $\mathbf{S} = \partial \boldsymbol{y}/\partial \boldsymbol{x}$ is obtained from equation (9). Matrix $\mathbf{S}$ can then be used in equation (6) to evaluate the $\mathrm{d}\gamma/\mathrm{d}\boldsymbol{x}$ vector needed for the sensitivity vector, $\boldsymbol{s}$, of equation (5).

A more efficient numerical process is the adjoint sensitivity method (ASM), which overcomes some inherent difficulties of the SDA and skips the evaluation of $\mathbf{S}$ [**9**, **10**]. A set of equations adjoint to equation (9) is defined:

$$\mathbf{A}^* \boldsymbol{s}^* = \boldsymbol{C}^* \tag{10}$$

where $\boldsymbol{s}^*$ is the adjoint function vector, $\mathbf{A}^*$ is the adjoint matrix, such that $\mathbf{A}^* = \mathbf{A}^{\mathrm{T}}$, and the vector $\boldsymbol{C}^*$ is selected to be

$$\boldsymbol{C}^* = \left(\frac{\partial \gamma}{\partial \boldsymbol{y}}\right)^{\mathrm{T}} \tag{11}$$

Using the definition of the adjoint matrix $\mathbf{A}^*$, the identity $\mathbf{C}^{\mathrm{T}} \boldsymbol{s}^* = (\boldsymbol{C}^*)^{\mathrm{T}} \mathbf{S}$ is derived, and equation (6) can then be expressed in terms of the adjoint matrix and vectors:

$$\left(\frac{\mathrm{d}\gamma}{\mathrm{d}\boldsymbol{x}}\right) = \left(\frac{\partial \gamma}{\partial \boldsymbol{x}}\right) + (\boldsymbol{C}^*)^{\mathrm{T}} \cdot \mathbf{S} = \left(\frac{\partial \gamma}{\partial \boldsymbol{x}}\right) + \mathbf{C}^{\mathrm{T}} \cdot \boldsymbol{s}^*$$

$$= \left(\frac{\partial \gamma}{\partial \boldsymbol{x}}\right) + \mathbf{C}^{\mathrm{T}} (\mathbf{A}^{\mathrm{T}})^{-1} \boldsymbol{C}^*$$

Once the terms of the sensitivity vector have been derived, it is possible to study the sensitivity of the seal operation to changes in both the design parameters and the possible control variables about the desired working point $(\boldsymbol{x}^{\mathrm{o}}, \boldsymbol{y}^{\mathrm{o}})$. For different working points, a different $\boldsymbol{s}$ has to be calculated.

The above sensitivity study also enables the estimation of the overall steady state misalignment in the presence of small disturbances or changes in the operational variables at each working point. If the working point and the design point are identical, the manufacturing tolerances may be included in the estimation:

$$\gamma' = \gamma + \sum_{j=1}^{m} \left(\frac{\mathrm{d}\gamma}{\mathrm{d}x_j}\right)_{(\boldsymbol{x}^{\mathrm{o}}, \boldsymbol{y}^{\mathrm{o}})} \Delta x_j + O(\Delta x_j^2) \tag{13}$$

where γ' is the final misalignment obtained owing to the changes (and tolerances) Δx_j in the corresponding x_j variables. The derivatives in the brackets are obtained from the sensitivity definition in equation (12).

3 COMPUTATIONAL EXAMPLE

In this study the analysis is applied to an existing test rig, similar to the scheme in Fig. 1. It is equipped with proximity sensors to measure the gap between the seal faces and an air pressure control chamber inside the FMR intended to vary the axial load (closing force) and maintain a desired gap. The geometry of the FMR test rig is fixed and the lubricant is water. The dimensional input variables to the system and their values or range of values are given in Table 1.

For the seal used in this study $R_{\mathrm{i}} = 0.8$ and, therefore, $\gamma_{\mathrm{cr}} = 1.25$, according to equation (4). Thus, to avoid seal face contact, the normalized relative misalignment between the rotor and the stator should be kept below this value.

The effect of the input parameters on the maximum normalized relative misalignment was studied by Zou *et al.* [**6**] who calculated this misalignment for the range of parameters given in Table 2. Results are presented in a set of graphs depicting γ versus β^* for different clearances and for different combinations of ΔP_{oi} and ω. A qualitative feel for the sensitivity to parameter changes of each working point can be obtained by observing the slope of the curves at this point.

An alternative presentation is given in Fig. 2, where results for γ are plotted for all 18 000 possible combinations of these parameters (within the resolution specified in Table 2) as a function of the coning angle β^*. These results are clustered in ten major groups for the different β^* within one mrad from each other; each group contains five subgroups for β^* within 0.2 mrad

Table 2 Variables affecting the misalignment and the studied range

Variable and units	Range studied	Resolution	Number of cases
Coning angle β^* (mrad)	0.2–10	0.2	50
Pressure ΔP_{oi} (kPa)	100–900	100	9
Clearance C_{o} (μm)	2–10	2	5
Speed ω (rad/s)	80–360	40	8

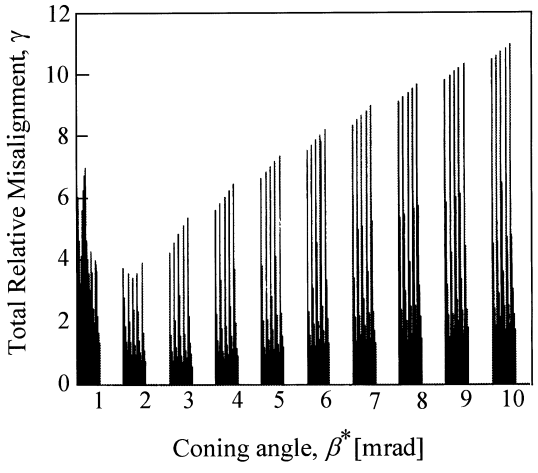

Fig. 2 Total relative misalignment for all the studied cases

of each other. Each subgroup is further divided into nine groups of different ΔP_{oi} values, and, subsequently, each of these contains the data for five different clearances and eight shaft speeds. Although the division into groups is somewhat arbitrary, Fig. 2 indicates that most of the smallest values for the normalized relative misalignment γ are grouped within the $\beta^* = 1.2$–2.0 mrad range.

Further zooming into Fig. 2 is demonstrated in Fig. 3 for $\beta^* = 1.2$–2.0 mrad, the minimal γ group. Figure 3a depicts the entire $\beta^* = 1.2$–2.0 mrad group, Fig. 3b concentrates on nine groups of pressures (100–900 kPa) for the $\beta^* = 1.2$ mrad group and Fig. 3c further zooms into the two extreme pressure groups, 100 and 900 kPa respectively, and shows the misalignment for the five different clearances. The top curves of the trapezoids in Fig. 3c describe the effect of the shaft speed.

Figures 2 and 3 can also be used to determine the non-contacting range of working points by drawing a horizontal line at the $\gamma = 1.25$ criterion, similar to the study by Zou *et al.* [6]. Any working point below this line is predicted to operate in non-contacting mode. Thus, the largest contiguous non-contacting range (NCR), in which it would be safe for this test rig to operate, is given by a seal having a coning angle between 1.2 and 4 mrad and maintained at any combination of pressures between 500 and 900 kPa (or higher), clearances from 2 to 8 μm and speeds anywhere between 80 and 360 rad/s. This range can be stretched to accommodate operation at certain different conditions at the expense of others.

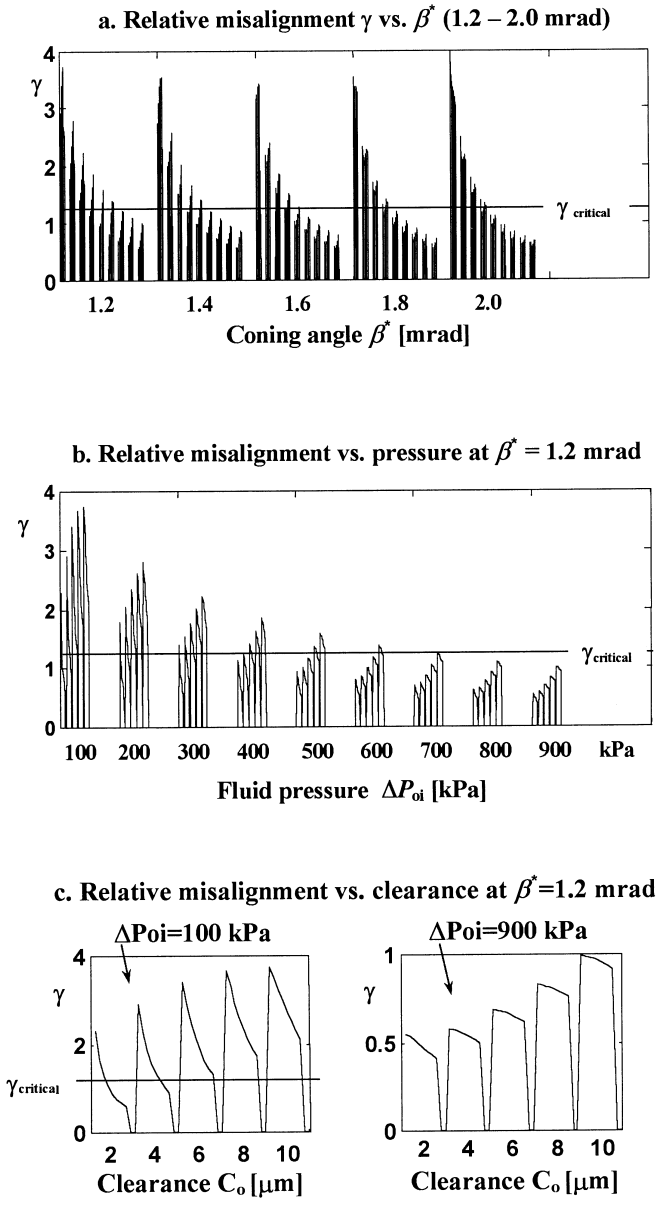

Fig. 3 Misalignment versus β^*, C_o and ΔP (zooming into $\beta^* = 1.2$–2.0 mrad group)

Next, the sensitivity study is applied to the test rig. Using the definitions of the input $\boldsymbol{x}$ and the governing equation $\boldsymbol{y}$ vectors, equations (3) and (2), respectively, the sensitivity vector $\boldsymbol{s}$ is calculated according to equation (5). Either the SDM or the ASM (both would yield identical results) can be used, with the latter resulting in fewer and faster computations. Table 3 summarizes the results for a particular working point of the test rig, given by $\omega = 180\,\text{rad/s}$, $C_o = 6\,\mu\text{m}$, $\Delta P_{oi} = 600\,\text{kPa}$ and $\beta^* = 1.2\,\text{mrad}$.

The left-hand side of the table (columns 1 to 4) provides the input variables and the corresponding sensitivities of γ and γ^* to these variables, i.e. the normalized $\boldsymbol{s}$ vector and the $\vec{\boldsymbol{s}}$ vector respectively. The right-hand side (columns 5 and 6) summarizes the resulting dependent variables, their values and the calculated values of the misalignment at this particular working point. The sensitivity values may be positive or negative. The larger the absolute value of the sensitivity coefficient, the larger is the sensitivity. The sign denotes the direction of the change in γ. For example, a 10 per cent increase in ω will cause a decrease of about 17 per cent in γ ($s_\omega = -1.71$). For this particular example, the following conclusions are drawn:

1. The total misalignment at this working point is only moderately sensitive to the initial misalignment of the rotor and the stator ($s_{\gamma i} = 0.6, s_{\gamma s} = 0.4$). Nevertheless, the smaller these initial misalignments, the smaller is the final steady state total misalignment of the rotor (safer from a contact prevention point of view).
2. It has been shown already that the steady state misalignment is quite sensitive to changes in shaft speed, and increasing the shaft speed may reduce the misalignment and the danger of obtaining a contact by a factor of about 1.7 of the percentage speed change.
3. Change in the clearance between the faces has a relatively good effect on the dimensional misalignment ($s_{C_o} = 1.56$) but only a moderate effect on the normalized $\gamma\,(0.56)$.
4. The lubricant differential pressure in the seal has a moderate to good effect on the misalignment ($s_{\Delta P} = 0.8$). The higher the pressure, the smaller is the obtained misalignment.
5. Although geometrical parameters such as the seal radii may strongly affect the total misalignment ($s_{ro} = -6.54, s_{ri} = 3.25$), these are usually determined by other application dependent design factors. However, it is recommended to consider the direction in which they are affecting the misalignment during the design stage and exploit it if possible. For the test rig studied here, these were determined by other considerations and it was irrelevant to incorporate this factor in the design.
6. Changing the coning angle also has a moderate effect on the misalignment at this working point ($s_\beta = -0.4$). If seals with different coning angles were available, it would be advantageous to select one with higher β^*, which complies with the non-contacting criteria (see Figs 2 and 3).
7. Selecting fluid with higher viscosity only slightly improves the misalignment ($s_\mu = 0.2$).
8. Both transverse and polar inertia have very little effect (sensitivities of 10^{-3}) on the misalignment.

In order to find a working point that is 'most sensitive' or 'least sensitive' to changes in any of the operational variables, it is possible to run an optimization code and search for a maximum or a minimum of a norm calculated from the sensitivity coefficients of interest. For example, the most sensitive point for the three operational variables (ω, ΔP_{oi}, C_o), within the NCR of this example, can be found by defining and calculating the norm:

$$s^2_{\text{norm}} = \left[s^2_\omega + s^2_{C_o} + s^2_{\Delta P} \right] \tag{17}$$

and searching for its maximum (Fig. 4).

Table 3 Sensitivity coefficients for the test rig at a selected working point

Independent variable (IP) $\boldsymbol{x}$	Value of $\boldsymbol{x}$	Sensitivity coefficients for normalized γ: $\boldsymbol{s} = (\mathrm{d}\gamma/\gamma)/(\mathrm{d}\boldsymbol{x}/\boldsymbol{x})$	Sensitivity coefficients: $\vec{\boldsymbol{s}} = (\mathrm{d}\gamma^*/\gamma^*)/(\mathrm{d}\boldsymbol{x}/\boldsymbol{x})$	Normalized dependent variable $\boldsymbol{y}$	Value of $\boldsymbol{y}$
γ^*_{ri}	1.50e − 3	5.99e − 1	5.99e − 1	I	2.51e − 4
γ^*_s	1.00e − 3	4.01e − 1	4.01e − 1	I_z	4.35e − 4
ω	1.80e + 2	−1.71e + 0	−1.71e + 0	K_s	3.13e − 3
C_o	6.00e − 6	5.58e − 1	1.56e + 0	D_s	1.01e − 4
ΔP_{oi}	6.00e + 5	−7.95e − 1	−7.95e − 1	D_f	2.39e − 2
r_o	2.54e − 2	−6.54e + 0	−7.54e + 0	K_f	2.96e − 2
r_i	2.03e − 2	3.25e + 0	3.25e + 0	Working point	
β^*	1.20e − 3	−4.11e − 1	−4.11e − 1	misalignment	
μ^*	8.94e − 4	−2.01e − 1	−2.01e − 1	γ^*	2.238e − 4
I^*	3.75e − 4	4.04e − 3	4.04e − 3	γ	9.473e − 1
I^*_z	6.49e − 4	−7.00e − 3	−7.00e − 3		

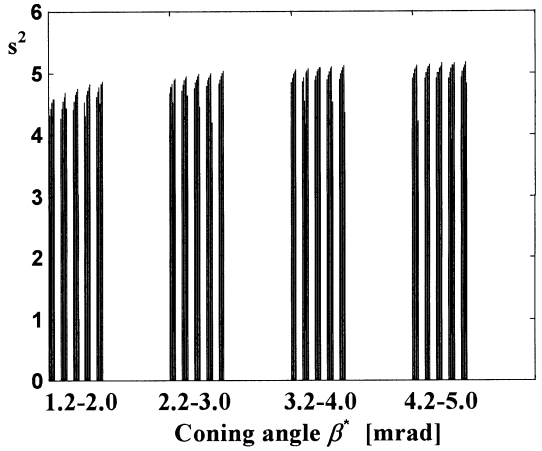

Fig. 4 Sensitivity norm for the non-contacting range of studied parameters

The s_{norm} as defined in equation (17) and shown in Fig. 4 is a compounded quantity and does not reveal which of its components contributes more than others. However, it indicates that, in general, the overall relative misalignment is slightly more sensitive at the higher coning angles considered (1–5 mrad). Because the difference in s^2 is marginal, it would still be preferable to control the operation of the seal about the minimal misalignment, i.e. a coning angle of 1.0–2.0 mrad. The exact working point is determined by studying the sensitivities of the misalignment to changes in the individual operational variables.

Figure 5 depicts the sensitivity of the maximum relative misalignment to changes in shaft speed, $s_\omega = \mathrm{d}\gamma/\mathrm{d}\omega$, for several coning angles (1–4 mrad), speeds (80–360 rad/s), clearances (2, 6, 10 μm) and pressures (500, 900 kPa). These sensitivities are always negative, implying reduction in misalignment for increase in speed. The absolute expected change in misalignment is quite high, displaying factors of 1.2–1.9. Raising pressure from 500 to 900 kPa increases the absolute sensitivity by 5–13 per cent. The sensitivities are higher at lower speeds, especially if the coning angles are small (1–2 mrad), but the difference disappears at about 3–4 mrad. At small clearances (2 μm) the spread between the sensitivities at $\beta^* = 1$ mrad reaches values of 0.5–0.6, but it shrinks to less than 0.1 for high clearances (10 μm).

Figure 6 depicts the sensitivity of the maximum relative misalignment to changes in clearances, $s_C = \mathrm{d}\gamma/\mathrm{d}C_o$, for the same studied NCR of coning angles (1–4 mrad), speeds (80–360 rad/s) and pressures (500, 700, 900 kPa). Clearances studied were 2, 4, 6, 8 and 10 μm. The sensitivities, s_C, may change sign and become negative, particularly at low clearances (2–6 μm) and higher coning angles. If clearance control were sought, as suggested by Zou and Green [**5**] and by Zou *et al.* [**6**], it would be desirable to obtain positive sensitivities; i.e. closing the gap would also reduce the misalignment. Therefore, it would be advantageous to work with a seal having a low coning angle (1–2 mrad or lower). Higher sensitivity would be obtained while maintaining the clearance at 4 μm or more, but then the misalignment itself would be increased. Pressure has only a small effect on s_C (looking at vertical changes in Fig. 6), but higher shaft speeds increase the absolute sensitivities (horizontal changes in Fig. 6). At 360 rad/s it is possible to maintain clearance as small as 2 μm (β^* of 1.5 mrad and lower) and still obtain positive s_C. Therefore, for clearance control to be effective, high speed should be maintained in order to allow for small clearances. Otherwise, relatively large leakage has to be tolerated. At high speeds, the spread between the sensitivity lines for different clearances is reduced, making it more attractive to work at small clearances. It should be noted, however, that excessively small clearances should be avoided while operating with seals having $\beta^* >$ 3–4 mrad (also not desirable from the leakage point of view), because of possible violation of the critical misalignment criterion. Moreover, at these coning angles the clearance control becomes much less sensitive.

Figure 7 depicts the sensitivity of the maximum relative misalignment to changes in pressure, $s_P = \mathrm{d}\gamma/\mathrm{d}P_{oi}$, for the above-mentioned range. Pressures between 500 and 900 kPa spaced by 100 kPa were examined. Similar to s_ω, the sensitivities s_P are also always negative, implying reduction in misalignment for increase in pressure. The absolute sensitivities are between 0.2 and 0.9 at the studied range. Raising pressure from 500 to 900 kPa increases the absolute sensitivity by 10–15 per cent. Working at high speeds (360 rad/s) and low coning angles (1–1.5 mrad) may result in a 20–25 per cent reduction in the absolute sensitivity factor. However, the sensitivities at the higher β^*(4 mrad) are almost unaffected by any of the studied parameters, remaining at about 0.85–0.95. Clearances have somewhat mixed effects on s_P. At 2 μm the sensitivities are low, especially at low pressures of 500–600 kPa. These increase slightly for 6 μm but drop again for 10 μm. Therefore, if pressure is used as the sole control variable, it would be best to work with a seal having a coning angle of 2–3 mrad or even higher. At these coning angles, s_P reaches its maximum (about 0.9) and is not sensitive to any of the operational variables.

4 CONTACT CONTROL

The above parametric study helps in determining the necessary conditions (coning angle and operation parameters) under which the seal will operate safely. It also helps in forming the strategy for actively controlling the seal and preventing contact.

Zou and Green [**5**] studied the possibility of eliminating seal contact by controlling the gap between the

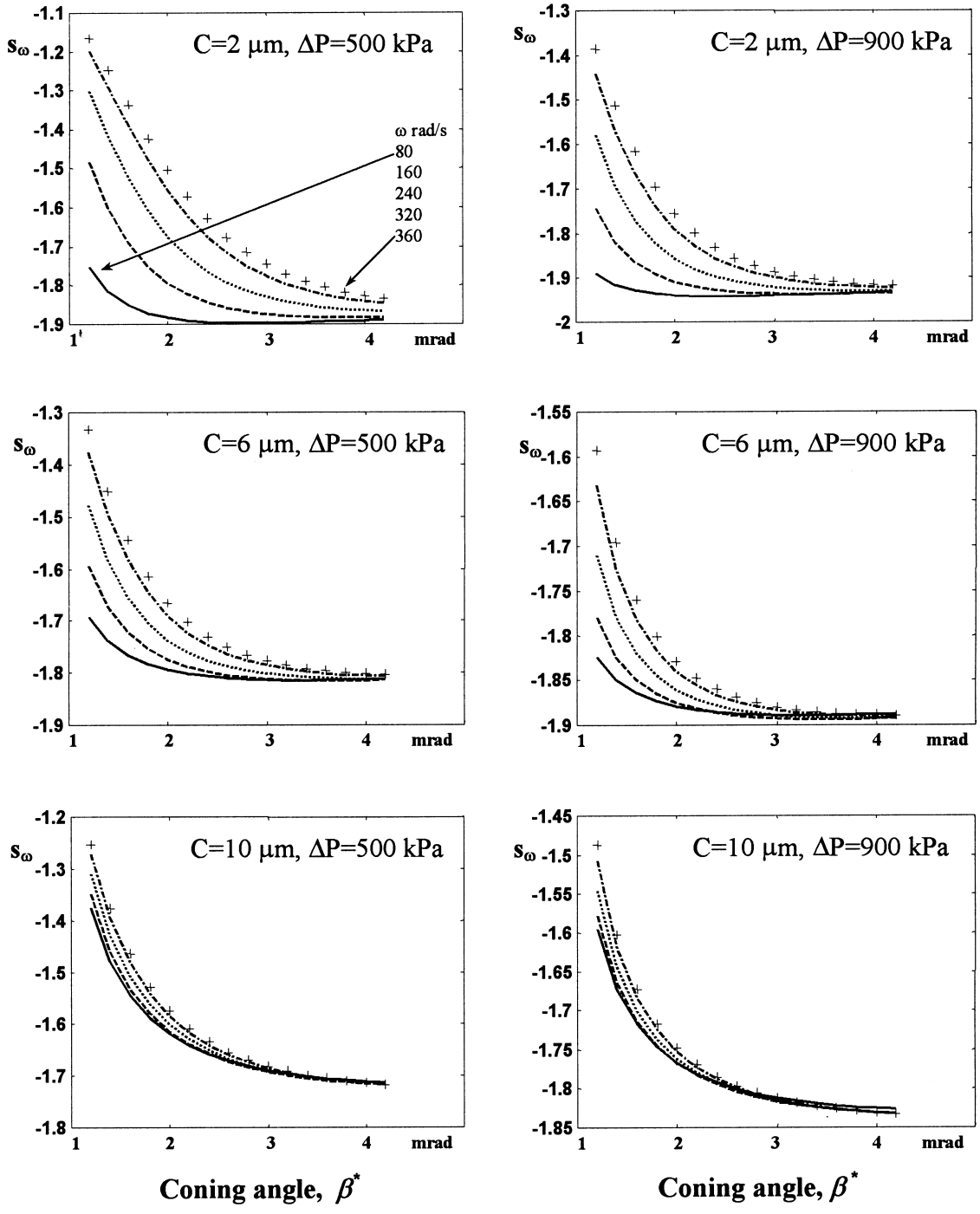

Fig. 5 Sensitivity of the maximum relative misalignment to changes in shaft speed

stator and the rotor faces. For the described test rig and from the minimum control effort point of view, it would be best to control the gap where it is most sensitive to clearance variations, i.e. at $\max\{|s_{C_o}|\}$ within the NCR. Leakage has to be taken into account in real application for final determination of the controlled clearance, as contradiction may evolve. It would be advantageous to have a seal with a small coning angle ($\beta^* = 1$–3 mrad or smaller), providing steady state with minimal misalignment (Fig. 2). At this working point the control should maintain a gap of $C_o = 4$–$6\,\mu$m (smaller gaps have other advantages but lose sensitivity). Neither the pressure nor the speed (at any $\Delta P_{oi} > 500$ kPa and ω in the studied range) affects the sensitivity very much at these gaps,

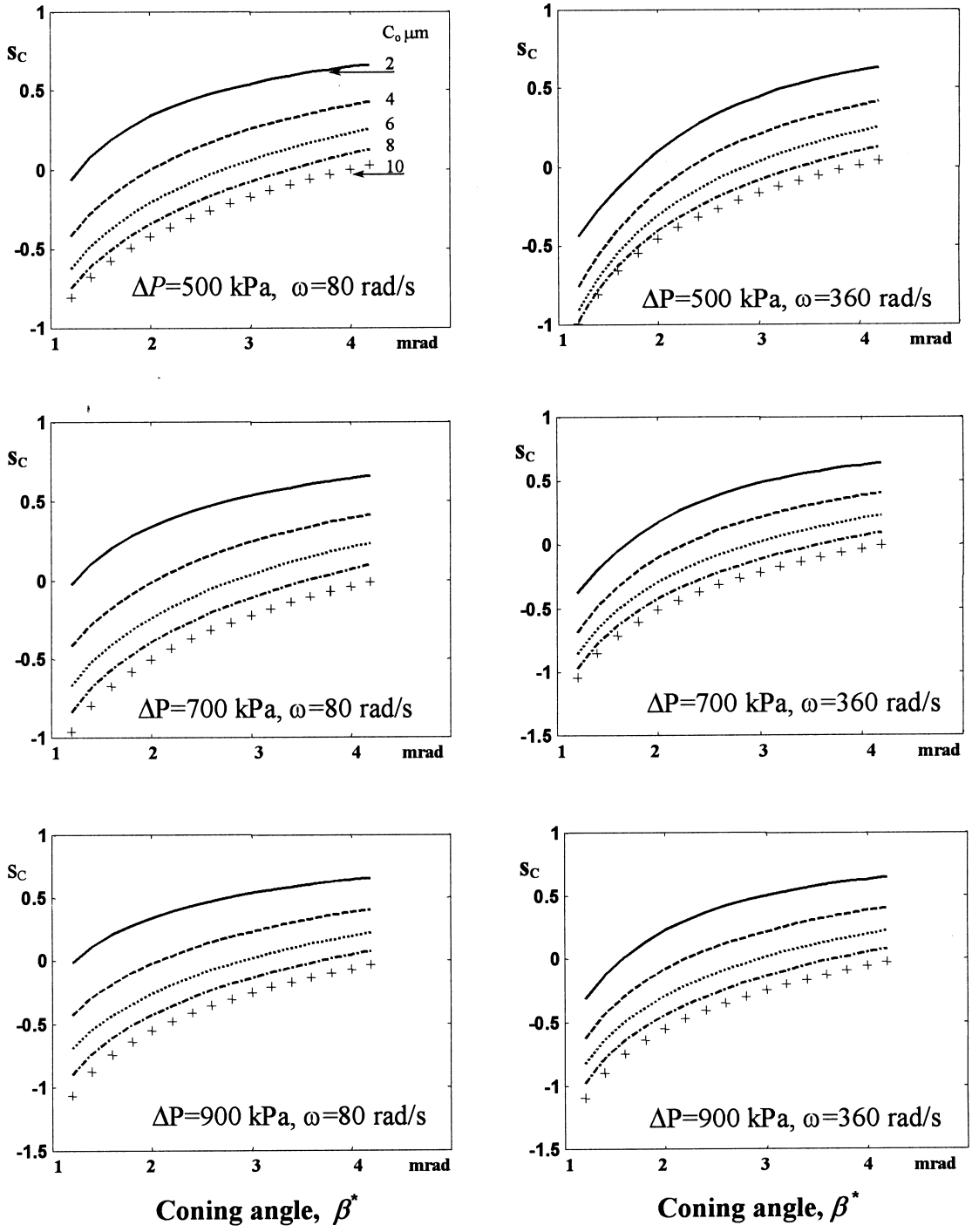

Fig. 6 Sensitivity of the maximum relative misalignment to changes in clearances

and this working point provides the highest possible s_C for this rig (Fig. 6). However, if leakage has to be minimized and a smaller gap is desired, somewhat less sensitive control is still possible while maintaining high speed.

Contrary to intuition, if face seal contact is caused by large relative misalignment, the control action should push the faces towards each other, closing the gap and further reducing the relative misalignment γ, because the sign of the sensitivity of γ with respect to C_o is positive. Similarly, if contact is controlled by any of the other operational variables, the best results are obtained if the

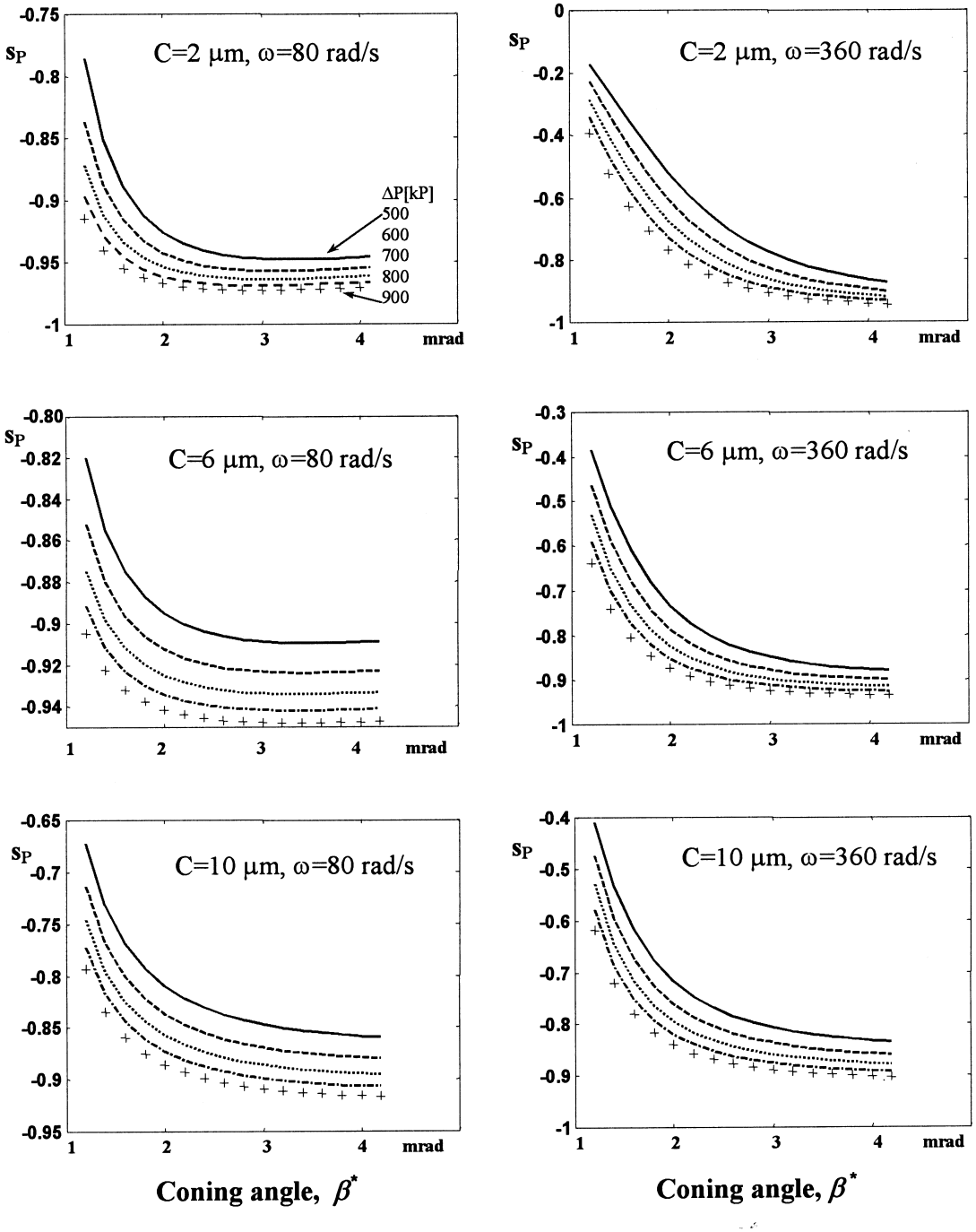

Fig. 7 Sensitivity of the maximum relative misalignment to changes in pressure

steady state operation, i.e. the reference point for the controlling variable, is as close as possible to where γ is small and is most sensitive to variation in this particular manipulated variable.

5 CONCLUSIONS

Contact should be eliminated in operation of non-contacting mechanical face seals. A proper working point can be selected for three different cases: for a common application with small load/speed and disturbances expected; for a limited variation case, where the changes are bound; and for a sensitive case with large, possibly unbounded changes. For the first two cases a proper design should minimize leakage (small β^* and C_o) and provide robustness to the varying conditions, namely insensitivity to the expected variations. For the third case, where large changes are expected and the application is particularly sensitive, an active control must be

designed and integrated with the operation of the seal. It is then possible to control the seal misalignment by one or more of the operational variables, shaft speed, fluid pressure and clearance. Selecting the working point for the active control option should yield the highest sensitivity of γ to changes in the manipulated variable, provided the required operational limits are met.

ACKNOWLEDGEMENTS

The authors wish to express their appreciation to the Office of Naval Research for the support of Research Grant N00014-95-1-0539, for Program 'Integrated Diagnostics'. Dr Peter Schmidt serves as Program Officer. This project is also supported in part by a Georgia Tech Foundation Grant, E25-A77, made by Mr Gilbert Bachman. This support is gratefully acknowledged.

REFERENCES

1 **Green, I.** Gyroscopic and support effects on the steady-state response of a noncontacting flexibly-mounted rotor mechanical face seal. *Trans. ASME, J. Tribology*, 1989, **111**, 200–208.

2 **Green, I.** and **Etsion, I.** Fluid film dynamic coefficients in mechanical face seals. *Trans. ASME, J. Lubric. Technol.*, 1983, **105**(2), 297–302.

3 **Green, I.** Gyroscopic and damping effects on the stability of a noncontacting flexibly mounted rotor mechanical face seal. *Dynamics of Rotating Machinery* (Eds J. H. Kim and W.-J. Yang), 1990, pp. 153–173 (Hemisphere).

4 **Green, I.** The rotor dynamic coefficients of coned-face mechanical seals with inward or outward flow. *Trans. ASME, J. Tribology*, 1987, **109**(1), 129–135.

5 **Zou, M.** and **Green, I.** Real-time condition monitoring of mechanical face seal. In Proceedings of 24th Leeds–Lyon Symposium on *Tribology*, London, Imperial College, 4–6 September 1997, pp. 423–430.

6 **Zou, M., Dayan, J.** and **Green, I.** Parametric analysis for contact control of a noncontacting mechanical face seal. In *Proceedings of Vibration, Noise and Structural Dynamics '99*, Venice, Italy, 1999, pp. 493–499.

7 **Lee, A. S.** and **Green, I.** Higher harmonic oscillations in a noncontacting FMR mechanical face seal test rig. *Trans. ASME, J. Vibr. and Acoust.*, 1994, **116**(2), 161–167.

8 **Lee, A. S.** and **Green, I.** Physical modeling and data analysis of the dynamic response of flexibly mounted rotor mechanical seal. *Trans. ASME, J. Tribology*, 1995, **117**(1), 130–135.

9 **Cacuci, D. G.** Sensitivity theory for non-linear systems. *J. Math. Phys.*, 1981, **22**, 2794–2812.

10 **Wacholder, E.** and **Dayan, J.** Application of the adjoint sensitivity method to the analysis of supersonic ejector. *Trans. ASME, J. Fluids Engng*, 1984, **106**, 425–429.

